Recovery of PEX1-Gly843Asp peroxisome dysfunction by small-molecule compounds

Rui Zhang[a], Li Chen[a], Sarn Jiralerspong[b], Ann Snowden[c], Steven Steinberg[c], and Nancy Braverman[b,1]

[a]McKusick-Nathans Institute of Genetic Medicine, The Johns Hopkins University, Baltimore, MD 21205; [b]Montreal Children's Hospital Research Institute, McGill University, Montreal, QC H3Z 2Z3, Canada; and [c]Department of Neurogenetics, Kennedy Krieger Institute, Baltimore, MD 21205

Zellweger spectrum disorder (ZSD) is a heterogeneous group of diseases with high morbidity and mortality caused by failure to assemble normal peroxisomes. There is no therapy for ZSD, but management is supportive. Nevertheless, one-half of the patients have a phenotype milder than classic Zellweger syndrome and exhibit a progressive disease course. Thus, patients would benefit if therapies became available and were instituted early. Recent reports indicate several interventions that result in partial peroxisome recovery in ZSD fibroblasts. To identify drugs that recover peroxisome functions, we expressed a GFP-peroxisome targeting signal 1 reporter in fibroblasts containing the common disease allele, PEX1-p.Gly843Asp. The GFP reporter remained cytosolic at baseline, and improvement in peroxisome functions was detected by the redistribution of the GFP reporter from the cytosol to the peroxisome. We established a high-content screening assay based on this phenotype assay and evaluated 2,080 small molecules. The cells were cultured in chemical for 2 days and then, were fixed and imaged by epifluorescent microscopy on a high-content imaging platform. We identified four compounds that partially recover matrix protein import, and we confirmed three using independent assays. Our results suggest that PEX1-p.G843D is a misfolded protein amenable to chaperone therapy.

Zellweger spectrum | AAA ATPase | misfolded protein | chemical screening | pharmacologic chaperone

The peroxisome biogenesis disorders, including Zellweger spectrum disorder (ZSD) and Rhizomelic chondrodysplasia punctata (RCDP), are a heterogeneous group of autosomal recessive diseases caused by mutations in *PEX* genes. Among the mutations identified in ZSD, the PEX1-p.Gly843Asp or G843D (c.2528G > A) founder allele occurs in high frequency in patients of European origin (1). The presence of at least one PEX1-p.G843D allele predicts a phenotype milder than classic Zellweger syndrome (ZS) (2). Overall, the milder phenotypes, neonatal adrenoleukodystrophy (NALD) and infantile Refsum disease (IRD), are associated with missense alleles in *PEX* genes, less severe biochemical deficiencies, and more functional peroxisomes, findings consistent with residual peroxin function.

When fibroblasts from NALD-IRD patients are cultured at 30 °C, peroxisome biogenesis improves. This was noted for cell lines with missense alleles in *PEX1* (G843D) (3), *PEX2* (E55K) (4), *PEX6* (G572I, I845T, L57P) (5, 6), *PEX26* (R98W, L45P) (7), and *PEX13* (I326T) (8) and suggests reduced protein misfolding at lower temperature (9). In contrast, ZS cell lines did not respond. These studies showed increased peroxisome number and improved import, matrix protein processing, very long chain fatty acid (VLCFA) oxidation, and plasmalogen biosynthesis. Overexpression of *PEX* missense alleles in CHO cells null for the corresponding peroxin conferred the temperature-sensitive phenotype, directly implicating the expressed protein in causing this phenotype (7).

Several groups have studied PEX1-p.G843D. Walter et al. (3) showed markedly reduced levels (5–15%) compared with wild-type PEX1 in fibroblast lysates from patients homozygous for this mutation and a 2- to 3-fold increase at 30 °C. Because *PEX1* transcript level in these patients is normal (10), it is likely that the PEX1-p.G843D is misfolded and degraded. PEX1 is an AAA (**ATPase associated with diverse cellular activities**) ATPase that oligomerizes with PEX6 AAA ATPase and when complexed to PEX26, recycles PEX5 from the peroxisome membrane to the cytosol (11). The interaction between PEX1-p.G843D and PEX6 is reduced to less than 70% of wild type (12). Peroxisome functions also recover when PEX6 is overexpressed in PEX1-p.G843D cells, consistent with conformational rescue by a binding partner (12). Finally, when ZSD fibroblasts, including those containing PEX1-p.G843D, are cultured in 4-phenylbutyrate, peroxisome numbers increase 2- to 3-fold and functions improve (13). Overall, these observations suggest that patient defects are amenable to intervention at the cellular level and implicate peroxin stabilization and peroxisome proliferation as mechanisms that drugs could recapitulate. We sought to develop a high-throughput assay to screen small-molecule libraries and identify drugs that may be further developed into clinical therapy. Identified compounds can serve as starting points for the development of others with optimal pharmacologic profiles.

Results

Development of a High-Throughput Assay. We chose to test PEX1-p.G843D, a missense allele rescued by the mechanisms discussed and accounting for one-third of all ZSD alleles. To monitor PEX1 function, a primary cell line, heterozygous for the common PEX1 alleles p.G843D and I700fs, was transformed, immortalized, and transfected with a GFP-peroxisome targeting signal 1 (PTS1) reporter. A stable clone was selected; we refer to these cells as PEX1-G843D-PTS1, because the second allele is null (10). We verified that GFP-PTS1 remains predominantly cytosolic in these cells when cultured at 37 °C (Fig. 1, untreated). After 2 days at 30 °C, we observed redistribution of GFP-PTS1 from the cytosol to punctate structures, indicating recovery of PTS1 matrix-protein import (Fig. 1, 30 °C). Because lower temperature recovers matrix-protein import, we predicted that nonspecific chemical chaperones would also recover matrix-protein import. Chemical chaperones are small-molecule osmolytes, such as glycerol, DMSO, amino acids and trimethylamines, including **trimethylamine *N*-oxide (TMAO)**, and betaine (trimethylglycine). The mechanism for their chaperone function is unknown, but might include conformational correction and prevention of nonproductive protein interactions (14). To evaluate these chemicals, PEX1-G843D-PTS1 cells were seeded in 96-well plates and cultured at 37 °C. Chemical was added the next day, and after 2 days, we observed robust recovery of punctate GFP-PTS1 in 3% DMSO, 200 mM TMAO, 5% glycerol, 100 mM betaine, and 300 mM proline
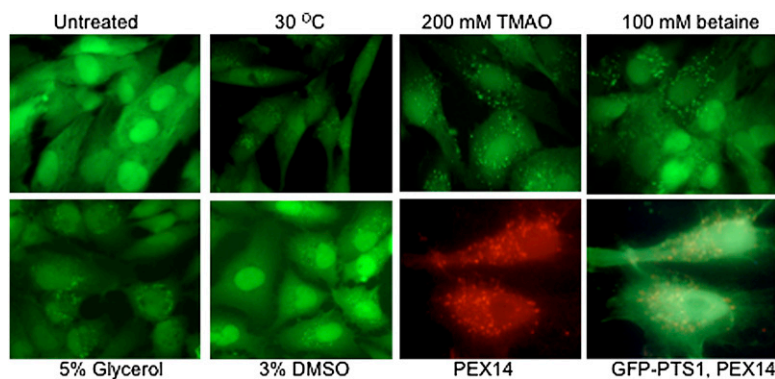
Fig. 1. Response to nonspecific chemical chaperones in PEX1-G843D-PTS1 cells. Cells were cultured for 2 days at 30 °C or 37 °C with chemical and imaged live (30 °C; glycerol and DMSO) or after fixation (the remainder). Note the redistribution of GFP-PTS1 from the cytosol to the peroxisome in the treated groups; results were similar for 300 mM proline. In the lower right two images, cells cultured in TMAO were permeabilized and incubated with PEX14 antiserum and Texas Red conjugated secondary antibody. Colocalization of PEX14 and GFP is shown in the last image.

(Fig. 1). To confirm that the punctate structures were peroxisomes, we performed indirect immunofluorescence (IF) with antiserum to the membrane peroxin, PEX14, and all punctate GFP structures colocalized with peroxisome membranes (Fig. 1 GFP-PTS1, PEX14).

To show that recovery of GFP-PTS1 targeting is a reliable indicator of the recovery of functional peroxisomes, we evaluated peroxisome functions by three independent assays. First, we evaluated the recovery of endogenous matrix protein import by IF using primary fibroblasts homozygous for PEX1-p.G843D. Cells were cultured at 37 °C in glycerol and TMAO or at 30 °C without chemicals for 2 days. Then, they were fixed, permeabilized, and incubated with antiserum to the PTS2 matrix protein (thiolase) and catalase. Thiolase import enabled us to assess the competency of the PTS2 import pathway. Although catalase uses the PTS1 pathway, it is targeted less efficiently by its C-terminal variant, Ala-Asn-Lys-Leu, and therefore, it is a sensitive indicator of peroxisome deficiency. To document colocalization of matrix and membrane proteins, cells were coincubated with antiserum to PEX14 or PMP70. We determined the number of cells with more than 20 importing peroxisomes and reported this in Table 1 as a percentage of the total number of cells counted. We observed minimal import of thiolase and catalase in untreated cells, but substantial improvement was seen when cells were cultured at 30 °C or at 37 °C with chemical chaperones. We also evaluated the recovery of plasmalogen synthesis in primary fibroblast cell lines, two PEX1-p.G843D/null and one PEX1-p.G843D homozygote, with nonspecific chemical chaperones or at 30 °C (Table 1, last column). For each condition, plasmalogen biosynthesis improved significantly compared with the untreated results.

Finally, we evaluated the recovery of PTS2 protein processing by immunoblotting (Fig. 2). Mammalian PTS2 proteins are thiolase, phytanoyl-CoA hydroxylase (PhyH), and alkylglycerone phosphate synthase (AGPS). After import of these preproteins, a PTS1 matrix protease removes the N-terminal PTS2 sequence, generating a smaller, mature protein (15). The relative increase in this maturation step should reflect the recovery of both PTS1 and PTS2 import observed in the previous experiments. PEX1-p.G843D primary fibroblasts were incubated for 2 days with nonspecific chaperones, and immunoblotting was performed on whole cell lysates. Results were interpreted by comparing the amounts of unprocessed to mature protein in untreated and treated samples. We observed a relative increase in the 42-kD mature thiolase in TMAO, glycerol, and betaine treated cells compared with untreated cells (Fig. 2*A*, lanes 2 and 7 compared with lane 1 for *PEX1*-643 and *PEX1*-214 and Fig. 2*B*, lane 8 compared with lane 1 for *PEX1*-214). Similarly, for *PEX1*-214, we observed an increase in the proportion of the 28-kDa mature PhyH in TMAO and betaine (Fig. 2*C*, lanes 2 and 8 compared with lane 1) and the 66-kDa AGPS in TMAO and glycerol (Fig. 2*D*, lanes 2 and 7 compared with lane 1). We conclude from these experiments that the redistribution of GFP-PTS1 from the cytosol to the peroxisome is a reliable indicator of the recovery of peroxisome functions. These results support the use of PEX1-G843D-PTS1 cells in a high-throughput phenotype screen to identify additional small-molecule compounds.

Table 1. Functional recovery in PEX1-G843D primary fibroblasts cultured in chemical chaperones

| Treatment | Number of importing cells/total cells counted* | | Plasmalogen biosynthesis[†] |
	Thiolase (PTS2)	Catalase (PTS1)	$^3H/^{14}C$ (nl < 0.7)
Untreated	26/500 (5%)	6/510 (1%)	2.26 ± 0.46
30 °C	143/200 (71%)	54/207 (26%)	0.98 ± 0.20 (P = 0.018)
200 mM TMAO	257/300 (86%)	40/200 (20%)	1.15 ± 0.18 (P = 0.016)
5% glycerol	105/200 (53%)	45/181 (25%)	1.24 ± 0.27 (P = 0.022)
100 mM betaine	100/140 (71%)	46/172 (27%)	

*PEX1-643 (G843D/G843D). Experiments were performed in triplicate, and results were pooled.
[†]PEX1-708 (G843D/E972fs), PEX1-706 (G843D/I700fs), and PEX1-643. Each cell line was tested in duplicate three times. We reported mean and SD of the pooled treatment results. P value was obtained by unpaired Student t test. Baseline plasmalogen synthesis was PEX1-708 (1.68), PEX1-706 (2.21), and PEX1-643 (2.27). Note that lower values represent more normal plasmalogen synthesis.
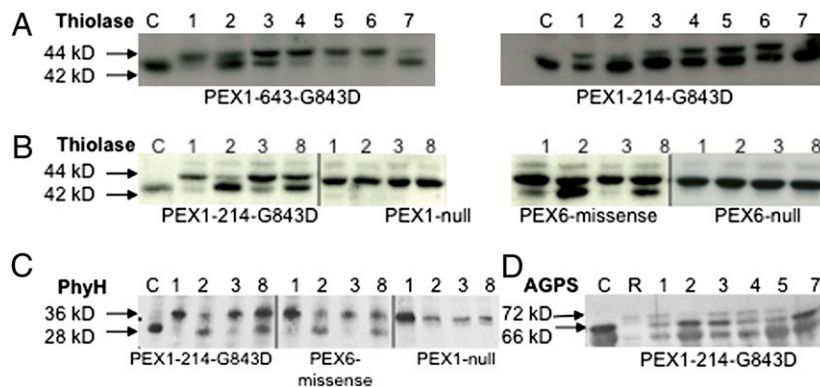
Fig. 2. Chemical treatment rescues PTS2 processing in PEX1- and PEX6-deficient primary fibroblasts. (*A*) Recovery of 42-kDa thiolase in two PEX1-G843D homozygous cell lines. (*B*) Recovery of 42-kDa thiolase in PEX1-G843D vs. PEX1 null cells is shown on the left, and PEX6 missense vs. null cells are shown on the right. (*C*) Recovery of 28 kDa PhyH in PEX1-G843D, PEX6 missense, and PEX1 null cells. (*D*) Recovery of 66 kDa AGPS in PEX1-G843D cells. Lane C, control; lane 1, untreated; lane 2, 200 mM TMAO; lane 3, 10 μM AD; lane 4, 10 μM Epicholestanol; lane 5, GF109203x 3 μM; lane 6, Ro31-8220 0.5 μM; lane 7, 5% glycerol; lane 8, 100 mM betaine; lane R, RCDP1 cells that were unable to import AGPS, which highlights the absence of the band corresponding to 66 kDa AGPS. Genotypes: PEX1 null-I700fs/I700fs, PEX6 null-802_815del/802_815del, and PEX6 missense-R60Q/R812W.

Chemical Library Screening. For the assay, we seeded 96-well plates with PEX1-G843D-PTS1 cells and added chemicals the next day. Each plate contained 80 wells with experimental compounds at 10 μM and had eight negative (DMEM or DMSO) and positive (TMAO or glycerol) controls. In total, 2,080 experimental compounds were screened in duplicate. The plates were cultured at 37 °C for 48–56 hours and then were fixed and incubated with DAPI nuclear stain to assist image focus; 3 × 3 montage images were obtained for each well and evaluated by visual inspection, and 200–300 cells/well were reviewed to determine the number of cells with >20 punctate structures, or importing peroxisomes, per cell. We reported this as the percent of importing cells. Importing cells ranged from 0% to 2% in the negative control wells and 70% to 100% in the positive controls. When duplicate wells showed >20% importing cells, we considered this a hit compound. With this methodology, we identified four hit compounds: acacetin diacetate (AD) and epicholestanol, in which 45% and 30% of cells recovered punctate structures, respectively, and PKC inhibitors, GF109203x and Ro31-8220, in which there was 60% and 65% recovery, respectively. Fig. 3 shows representative images from the library screen, including those from the four hits. Because GF109203x and Ro31-8220 exhibited cytosolic red autofluorescence (16), we reviewed these images carefully but did not observe any bleed of the autofluorescence into the GFP channel. AD and the PKC inhibitors were retested at 5, 10, and 20 μM. A dose-dependent response was observed, and more positive cells were observed at 20 μM than at 5 μM.

Confirmation of Chemical Activity. To confirm that the identified compounds improve peroxisome functions, we performed additional experiments in primary cell lines homozygous for PEX1-p. G843D and cultured in chemical for 2–3 days. Using IF, we observed improvement in catalase and thiolase import in 10 μM AD and 20 μM epicholestanol; 10 μM GF109203x and Ro31-8220 caused high cell death in primary fibroblasts and thus, were used at 0.5–3 μM. Representative images are shown in Fig. S1, and the proportion of cells showing rescue of import is listed in Table 2. Plasmalogen synthesis improved in PEX1-p.G843D homozygous cell lines cultured in the two PKC inhibitors, AD and an analog (acacetin), but not in epicholestenol. Epicholestenol was tested in duplicate one time; untreated cells showed ^{3}H/^{14}C levels of 1.1 and 1.2 compared with levels of 0.98 and 0.97 in treated cells.

To evaluate the recovery of N-terminal processing of thiolase, we performed immunoblotting of whole cell lysates from PEX1-p. G843D homozygous cells cultured in each compound (Fig. 2*A*).
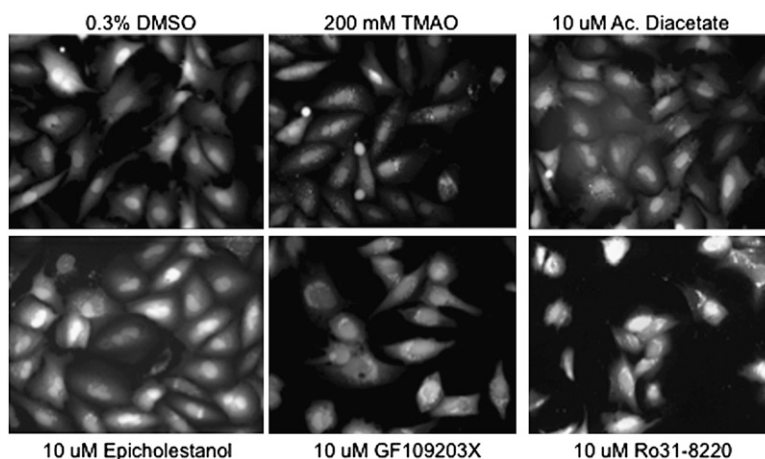

Fig. 3. One section of each montage, obtained in the high-throughput screen, is shown in the GFP channel. Compared with the cells in 0.3% DMSO solvent, there is a higher proportion of cells with punctate structures, representing importing peroxisomes, in the hit compounds and TMAO.

Compared with untreated cells (lane 1), there was relatively more mature thiolase in AD (lane 3) but not in epicholestanol (lane 4), GF109203x (lane 5), or Ro31-8220 (lane 6). To show that this effect required PEX1 protein, we repeated the experiment using a *PEX1* null cell line and found no improvement in thiolase processing after culture in TMAO, AD, and betaine (Fig. 2*B*, see PEX1 null in lanes 2, 3, and 8, respectively). Considering that PEX1 peroxin interacts with PEX6, also an AAA ATPase, we determined if AD might also recover peroxisome functions in *PEX6* defective cell lines. Thus, we evaluated the recovery of thiolase processing in *PEX6* missense and null cell lines. As shown in Fig. 2*B*, the *PEX6* missense cells did not respond to AD (lane 3) but responded to nonspecific chaperones, TMAO and betaine (lanes 2 and 8). The *PEX6* null cells were unresponsive to any chemical treatment (Fig. 2*B*). We next evaluated the processing of other PTS2-imported proteins, PhyH and AGPS (Fig. 2 *C* and *D*). *PEX1*-214 cells incubated in AD showed minimal improvement in PhyH and AGPS processing compared with untreated cells (Fig. 2 *C* and *D*, lane 3 compared with lane 1). There was no recovery of AGPS processing in epicholestanol and GF109203x (Fig. 2*D*, lanes 4 and 5) Again, the *PEX6* missense cell line did not respond to AD, and *PEX1* null cells did not respond to any treatment (Fig. 2*C*, center panels, respectively). Thus, the effect of AD is specific for PEX1-p.G843D cells, and it requires the presence of the PEX1 protein.

Finally, we evaluated the amounts of PEX1-p.G843D protein in *PEX1*-214 cells to determine if there was an increase in this unstable protein after treatment (Fig. 4*A*). As expected, we observed decreased PEX1 amounts compared with wild type but no obvious increase after chemical treatment. Because we were able to simultaneously reproduce the marginal increase in PEX1-p.G843D levels at 30 °C reported by other investigators (Fig. 4*A*, last two columns, 37 °C and 30 °C), we conclude that improvement of peroxisome functions by chemical treatment in these experiments was not accompanied by an obvious increase in PEX1-p.G843D protein levels. The amount of PEX6 protein was also decreased compared with control and was not increased in chemicals (Fig. 4*B*). We observed a small increase in PEX6 at 30 °C compared with 37 °C, which mirrored the response of the defective PEX1 peroxin. Because the PEX1-p.G843D substitution reduces the interaction between PEX1 and PEX6 (12), we infer that PEX6 is unstable without its partner, a conclusion supported by the absence of detectable PEX6 in yeast strains deleted for *PEX1* (17).

Discussion

Assay Utility. We have initiated a robust, high-throughput phenotype assay to identify therapeutic drugs for ZSD using an engineered cell line to detect redistribution of a PTS1 matrix protein reporter from the cytosol to the peroxisome. This redistribution, reflecting functional peroxisomal import, is a discrete and quantifiable molecular event that correlates to pathogenesis.
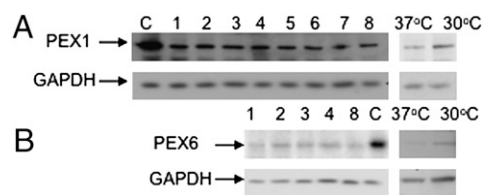

Fig. 4. PEX1 and PEX6 protein levels in *PEX1*-214 cells homozygous for G843D that do not recover with chemical treatment. Lanes C, control; lane 1, untreated; lane 2, 200 mM TMAO; lane 3, 3% DMSO; lane 4, 10 μM AD; lane 5, 10 μM Epicholestanol; lane 6, GF109203x 3 μM; lane 7, Ro31-8220 0.5 μM; lane 8, 5% glycerol, 37 °C and 30 °C. Note that PEX1 and PEX6 levels increase slightly at 30 °C. GAPDH was used to evaluate protein loading.

We confirmed a positive response by independent measurements in primary cell lines, which validate this approach for high-throughput screening. The confirmatory tests employed have a long track record, in our hands and those of multiple investigators, for accurately predicting peroxisome functions. Although the high-throughput images were scored by visual inspection, it is likely that larger library screens will require automated data analysis for reliable quantitative information.

In an initial screen of 2,080 bioactive compounds, we identified four that partially recover GFP-PTS1 matrix protein import. Treatment with AD recovers peroxisome functions in all three confirmatory assays. Treatment with PKC inhibitors resulted in recovery of peroxisome functions by both IF and plasmalogen biosynthesis. Treatment with epicholestenol, although showing some improvement by IF, was not otherwise confirmed. Our hit rate (compounds with the highest biologic activity) of 0.19% was within the range of other reports (18). An advantage of our assay is the detection of downstream effects, which should, theoretically, capture any mechanism of recovery, including unanticipated ones. Performing the assay in patient cell lines requires that the drug pass across at least one cell membrane and recover in vivo peroxisome functions. In addition, we showed recovery of peroxisome functions in fibroblasts from patients with either one or two PEX1-p.G843D alleles, suggesting that a significant number of ZSD patients are capable of responding to drug treatments.

Mechanism for Peroxisome Recovery in PEX1-p.G843D Cells. AAA ATPases contain one or two AAA cassettes, each with an ATP binding (Walker A) and ATP hydrolysis (Walker B) site. The functional unit is a hexamer that forms a double ring structure with the AAA domains stacked. Oligomerization is required for ATP binding and hydrolysis. Energy from ATP hydrolysis is converted into motion of the complex (19). PEX1 and PEX6 each contain two AAA domains and hetero-oligomerize. PEX26 recruits the AAA complex to the peroxisome by binding to the N terminus of PEX6 (20). Motion of the PEX1–PEX6 complex

Table 2. Functional recovery in PEX1-G843D primary fibroblasts cultured in hit chemicals

Treatment	Number of importing cells/total cells counted*		Plasmalogen biosynthesis[†]
	Thiolase (PTS2)	Catalase (PTS1)	$^3H/^{14}C$ (nl < 0.7)
Untreated	46/279 (16%)	47/259 (18%)	1.67 ± 0.34
10 μM acacetin diacetate	54/105 (51%)	69/165 (42%)	0.88 ± 0.12 ($P = 0.005$)[‡]
1 μM GF109203x	46/108 (46%)	97/196 (50%)	0.80 ± 0.37 ($P = 0.011$)
0.5 μM Ro31-8220	48/100 (48%)	52/129 (40%)	0.84 ± 0.32 ($P = 0.007$)[‡]
20 μM acacetin			1.16 ± 0.19 ($P = 0.04$)

*PEX1-214 (G843D/G843D). Experiments were performed in triplicate, and results were pooled.
[†]PEX1-643 and PEX1-503 (G843D/G843D). Each cell line was tested in duplicate three times. We report the mean and SD of the pooled treatment results. *P* value was obtained by unpaired Student *t* test.
[‡]For plasmalogen biosynthesis, we used 20 μM acacetin diacetate and 1 μM Ro31-8220.

Zhang et al.

recycles monoubiquitinated PEX5 from the peroxisome membrane to the cytosol. The different nucleotide states of PEX6 affect its binding and release from PEX26 (20).

Considering the multiple conformational states of the PEX1–PEX6–PEX26 complex, there should be several opportunities to influence folding intermediates in patients with missense changes in these proteins. For PEX1-p.G843D cells, recovery occurs at a lower temperature, reflecting improved folding at lower kinetic energy (9). In this paper, we showed that nonspecific chemical chaperones also rescued peroxisome functions. This recovery required some corresponding PEX1 protein, because it did not occur in *PEX1* null cells (Fig. 2 *B* and *C*). The lack of an observed increase in PEX1 levels (Fig. 4) with chemical compared with temperature rescue could be because of several reasons. There might be a small increase in PEX1 protein that is below the limit of detection but produces the observed functional effect. Alternatively, there could be two populations of PEX1, one that is completely misfolded and targeted for degradation and another that is not degraded but improperly folded and partially functional. Both populations can be rescued at lower temperature, but only the latter can be rescued by chemical treatment. Overall, we favor the hypothesis that recovery after drug treatment is based on conformational change of the PEX1 protein complex rather than changes in absolute levels of these proteins.

Potential Pharmacologic Chaperones for PEX1-p.G843D. Whereas chemical chaperones nonselectively stabilize mutant proteins, pharmacologic chaperones bind selectively to target proteins to stabilize their native state and/or facilitate the folding of nonnative intermediate states to the native state. Examples of drugs developed as pharmacologic chaperones include enzyme substrates or inhibitors, such as the iminosugar 1-deoxygalactonojirimycin (a reversible, competitive inhibitor of α-Gal A in Fabry disease) (21) and antagonists of the vasopressin V2 receptor in nephrogenic diabetes insipidus (22). The fact that these molecules could rescue different alleles of the same proteins shows that they are not necessarily mutation-specific molecules. Of the hits identified here, AD is a member of a large class of organic polyphenol compounds called flavonoids. An adult consumes around 200–300 mg of flavonoids per day, and they are considered safe nutrients (23). Flavonoids have been implicated as beneficial agents in various diseases (24, 25). The mechanisms responsible for their biologic effects include the ability to interact with and inhibit ATP binding cassette (ABC) transporters. This inhibition reduces drug resistance in cancer cells by diminishing the effect of these transporters as an efflux pump (26). Mechanisms could include competitive inhibition with the transported substance or to the nucleotide binding domain (NBD), suppressing ATP hydrolysis and energy-dependent drug efflux (27, 28). Flavonoids can also directly inhibit kinases, including protein kinase C, cyclin dependent kinase (CDK), and tyrosine kinases (29). Cocrystallization of flavonoids with CDK has shown that these compounds occupy the NBD (30). Recently, baicalein 5,6,7-tri methoxyflavone was shown to improve VLCFA oxidation in fibroblasts from patients with X-linked adrenoleukodystrophy (X-ALD) by indirectly stimulating peroxisomal fatty acid oxidation (31). Interestingly, the ABC transporters, ABCD2 and ABCD3, and acyl-CoA synthetases, SLC27A2 and SLC27A4 that contain an ATP/AMP binding motif, are potentially involved in the X-ALD phenotype. Thus, the improvement in peroxisomal VLCFA oxidation might be caused by a modifying effect of the drug at the NBD of these proteins.

The extensive literature showing flavonoids as ATP mimics alone supports their testing as candidate drugs in peroxisome disorders. The fact that they were identified here without bias provides strong support for this screening approach. In the current project, we found the flavone AD to be the most potent corrector of peroxisome functions in cells expressing PEX1-p.G843D. We propose that AD binds competitively and reversibly to ATP

binding sites or other locations on PEX1-p.G843D and acts as a pharmacologic chaperone. The observation of greater improvement in plasmalogen synthesis with AD compared with acacetin (Table 2, AD) suggests that the acetate groups enhance activity.

GF109203x (aminoalkyl bisindolylmaleimide) is a selective PKC inhibitor (IC_{50} 0.02 μM) and a competitive inhibitor with respect to ATP (K_i = 14 nM) (32). Ro 31–8220 is structurally similar. Like AD, we suggest that these drugs act as pharmacologic chaperones for PEX1-p.G843D by competitively binding at the ATP binding sites. However, because the concentrations used would be expected to also inhibit PKC, it is possible that this inhibition causes downstream effects that enhance peroxisome functions. Activated PKC phosphorylates PPARα, a transcription factor that induces a subset of peroxisome matrix enzymes (33). In addition, PKC phosphorylation activates phospholipase A2 to generate arachadonic acid and 1-alkyl- or 1-acyl-lysophospholipids from glycerophospholipids. Inhibition of PKC results in the inhibition of phospholipid hydrolysis (34) and could possibly result in the accumulation of plasmalogens as a secondary effect.

Future Work. There is currently no effective therapy for peroxisome biogenesis disorders, but management is supportive. The anticipated inclusion of peroxisomal disorders in expanded newborn screening programs presents a major challenge to uncover methods to delay the onset or progression of these disorders (35). We have shown that high-throughput drug screening in cultured patient cells can identify compounds that recover peroxisome functions. Larger compound libraries can now be screened after adaptation of imaging software. In addition, investigation of structure–activity relationships (SAR) for the confirmed hits could potentially generate a set of lead compounds that can be studied in animal models and eventually, clinical trials. Elucidation of the mechanism of action of these hit compounds promises to provide additional insight into peroxisome biology.

Materials and Methods

Cell Culture. Primary fibroblast cell lines, passage 5–15, were cultured at 5% CO_2, in DMEM with 10% (vol/vol) FBS. All patient samples received Institutional Review Board approved consent for use in research and were given Peroxisome Biogenesis Disorder numbers. *PEX1*-671 was transformed with SV40 large T antigen and immortalized with telomerase pBabePuro/hTERT (36). The subsequent cell population was transfected with pEGFP-PTS1 (Clontech), and single colonies were evaluated. A representative clone with medium GFP signal intensity and low punctate background was selected, and aliquots were frozen; one pellet was used for ~12 passages. When the proportion of GFP expressing cells was <95%, we reselected in G-418 (2 mg/mL) for 3 days. PCR amplification detected no mycoplasma genomes (37).

Chemicals. TMAO, DMSO, proline (Sigma-Aldrich), anhydrous betaine (Orphan Europe), and glycerol (Fisher Scientific) were obtained; 200 mM TMAO, 5% glycerol (vol/vol), and 3% DMSO (vol/vol) were dissolved in media, filter sterilized, and stored at −20 °C. Proline and betaine were dissolved in water, filter sterilized, and stored at 4 °C. The Spectrum Collection (MicroSource Discovery Systems Inc.) and Kinase Inhibitor Library (cat# 2832; BIOMOL) were obtained as 10 mM stock solutions in DMSO from the Johns Hopkins ChemCore. Hit chemicals were reobtained directly from the company. These were stored as 10 mM solutions in 100% DMSO at −20 °C; 1 mM epicholestanol was dissolved in 100% ethanol. The purity of AD was confirmed by mass spectroscopy.

High-Throughput Screening. Two thousand two hundred PEX1-G843D-PTS1 cells/well were seeded in BD Falcon 96-well collagen-coated imaging plates (cat# 353219). The plates were spun 500 × *g* for uniform cell distribution and cultured overnight, and chemicals were added the next day; 0.4 μL of 10 mM compound was dispensed robotically into 200 μL of culture medium for three rounds of side mixing before 100 μL was removed and added to each experimental well with two rounds of side mixing to give 10 μM final concentration in duplicate plates. Columns 1 and 12 were reserved for negative (DMEM or 0.3% DMSO) and positive (5% glycerol or 200 mM TMAO) controls, respectively. The barcoded plates were cultured at 5% CO_2 and 37 °C for 48–56 hours. The cells, generally 60–80% confluent, were washed, fixed with 3% formaldehyde, incubated in 5 μM Hoescht 33342 (Molecular

Probes), washed, and stored sealed at 4 °C in PBS up to 5 days. Plates were imaged on a BD Pathway 855 High-Content Bioimager (BD Biosciences). To set parameters, individual wells were reviewed, and focus was optimized on the DAPI (nuclear) images and refined on the GFP (cytosolic) images; exposure time and depth were determined. Montages (3 × 3) were obtained with a 20× objective under GFP and DAPI channels. Some wells were rescanned to improve focus or capture more cells. Images from some wells were lost because of drug toxicity.

Functional Assays. Fibroblasts were seeded to 50% (PEX1-G843D-PTS1) and 70% (primary cells) confluence in 25-cm² flasks or collagen-coated glass coverslips. Cells were cultured overnight and then incubated with chemical for 2 days. Chemicals were thawed at 22 °C, vortexed, diluted in media, vortexed, and sonicated for 15 seconds.

Indirect immunofluorescence. Cells were fixed, permeabilized, and incubated with antiserum as reported (38). Polyclonal rabbit PEX14, sheep PMP70 (S. Gould, Baltimore), and rabbit PEX6 (G. Dodt, Tübingen, Germany) antiserum were gifts. Polyclonal rabbit anti-thiolase and AGPS were generated by standard procedure (N. Braverman, Montreal). Monoclonal mouse PhyH antibody was generated by National Institutes of Health NeuroMab Facility at University of California, Davis, CA. Polyclonal sheep anti-catalase and secondary antibodies were purchased. Images were viewed with an Olympus BTX21 microscope and 60× oil objective.

Immunoblotting. Cells were collected in boiling Laemmli buffer by scraping and were boiled for 15 minutes; 10 mg protein/lane was loaded on 7.5–12.5% SDS/PAGE minigels and run at 170 V for 1 hour. Separated proteins were transferred to reinforced nitrocellulose membrane at 110 V and 4 °C. Membranes were blocked, hybridized with PEX6, thiolase, AGPS, PEX1 (611719; Becton-Dickinson), and GAPDH (1:7,500; 2118; Cell Signaling) antibodies, and visualized by ECL.

Plasmalogen biosynthesis. Cells were cultured for 18 hours before harvesting with substrates (^{3}H-hexadecylglycerol and ^{14}C-hexadecanol) and chemicals. Cells were resuspended in 0.5 mL water, sonicated, and stored at −20 °C. Plasmalogen synthesis was performed by TLC to comparing the microsomal incorporation of ^{3}H with the peroxisomal incorporation of ^{14}C (39).

1. Collins CS, Gould SJ (1999) Identification of a common PEX1 mutation in Zellweger syndrome. *Hum Mutat* 14:45–53.
2. Preuss N, et al. (2002) PEX1 mutations in complementation group 1 of Zellweger spectrum patients correlate with severity of disease. *Pediatr Res* 51:706–714.
3. Walter C, et al. (2001) Disorders of peroxisome biogenesis due to mutations in PEX1: Phenotypes and PEX1 protein levels. *Am J Hum Genet* 69:35–48.
4. Osumi T, et al. (2000) Temperature sensitivity in peroxisome assembly processes characterizes milder forms of peroxisome biogenesis disorders. *Cell Biochem Biophys* 32:165–170.
5. Raas-Rothschild A, et al. (2002) A PEX6-defective peroxisomal biogenesis disorder with severe phenotype in an infant, versus mild phenotype resembling Usher syndrome in the affected parents. *Am J Hum Genet* 70:1062–1068.
6. Imamura A, et al. (2000) Temperature-sensitive mutation of PEX6 in peroxisome biogenesis disorders in complementation group C (CG-C): Comparative study of PEX6 and PEX1. *Pediatr Res* 48:541–545.
7. Matsumoto N, et al. (2003) Mutations in novel peroxin gene PEX26 that cause peroxisome-biogenesis disorders of complementation group 8 provide a genotype-phenotype correlation. *Am J Hum Genet* 73:233–246.
8. Hashimoto K, et al. (2005) Molecular mechanism of a temperature-sensitive phenotype in peroxisomal biogenesis disorder. *Pediatr Res* 58:263–269.
9. Gregersen N, Bolund L, Bross P (2003) Protein misfolding, aggregation, and degradation in diseases. *Protein Misfolding and Disease*, eds Bross B, Gregersen N (Humana Press, Totowa, NJ), pp 3–17.
10. Maxwell MA, et al. (1999) A common PEX1 frameshift mutation in patients with disorders of peroxisome biogenesis correlates with the severe Zellweger syndrome phenotype. *Hum Genet* 105:38–44.
11. Platta HW, Debelyy MO, El Magraoui F, Erdmann R (2008) The AAA peroxins Pex1p and Pex6p function as dislocases for the ubiquitinated peroxisomal import receptor Pex5p. *Biochem Soc Trans* 36:99–104.
12. Geisbrecht BV, Collins CS, Reuber BE, Gould SJ (1998) Disruption of a PEX1-PEX6 interaction is the most common cause of the neurologic disorders Zellweger syndrome, neonatal adrenoleukodystrophy, and infantile Refsum disease. *Proc Natl Acad Sci USA* 95:8630–8635.
13. Wei H, Kemp S, McGuinness MC, Moser AB, Smith KD (2000) Pharmacological induction of peroxisomes in peroxisome biogenesis disorders. *Ann Neurol* 47:286–296.
14. Perlmutter DH (2002) Chemical chaperones: A pharmacological strategy for disorders of protein folding and trafficking. *Pediatr Res* 52:832–836.
15. Kurochkin IV, et al. (2007) Novel peroxisomal protease Tysnd1 processes PTS1- and PTS2-containing enzymes involved in beta-oxidation of fatty acids. *EMBO J* 26:835–845.
16. Brandt D, Gimona M, Hillmann M, Haller H, Mischak H (2002) Protein kinase C induces actin reorganization via a Src- and Rho-dependent pathway. *J Biol Chem* 277:20903–20910.
17. Platta HW, Grunau S, Rosenkranz K, Girzalsky W, Erdmann R (2005) Functional role of the AAA peroxins in dislocation of the cycling PTS1 receptor back to the cytosol. *Nat Cell Biol* 7:817–822.
18. Li JW, Vederas JC (2009) Drug discovery and natural products: End of an era or an endless frontier? *Science* 325:161–165.
19. Hanson PI, Whiteheart SW (2005) AAA+ proteins: Have engine, will work. *Nat Rev Mol Cell Biol* 6:519–529.
20. Tamura S, Yasutake S, Matsumoto N, Fujiki Y (2006) Dynamic and functional assembly of the AAA peroxins, Pex1p and Pex6p, and their membrane receptor Pex26p. *J Biol Chem* 281:27693–27704.
21. Benjamin ER, et al. (2009) The pharmacological chaperone 1-deoxygalactonojirimycin increases alpha-galactosidase A levels in Fabry patient cell lines. *J Inherit Metab Dis* 32:424–440.
22. Robben JH, Sze M, Knoers NV, Deen PM (2007) Functional rescue of vasopressin V2 receptor mutants in MDCK cells by pharmacochaperones: Relevance to therapy of nephrogenic diabetes insipidus. *Am J Physiol Renal Physiol* 292:F253–F260.
23. Aszalos A (2008) Role of ATP-binding cassette (ABC) transporters in interactions between natural products and drugs. *Curr Drug Metab* 9:1010–1018.
24. Marini H, et al. (2007) Effects of the phytoestrogen genistein on bone metabolism in osteopenic postmenopausal women: A randomized trial. *Ann Intern Med* 146:839–847.
25. Lin TS, et al. (2009) Phase II study of flavopiridol in relapsed chronic lymphocytic leukemia demonstrating high response rates in genetically high-risk disease. *J Clin Oncol* 27:6012–6018.
26. Katayama K, et al. (2007) Flavonoids inhibit breast cancer resistance protein-mediated drug resistance: Transporter specificity and structure-activity relationship. *Cancer Chemother Pharmacol* 60:789–797.
27. Trompier D, et al. (2003) Multiple flavonoid-binding sites within multidrug resistance protein MRP1. *Cell Mol Life Sci* 60:2164–2177.
28. Nissler L, Gebhardt R, Berger S (2004) Flavonoid binding to a multi-drug-resistance transporter protein: An STD-NMR study. *Anal Bioanal Chem* 379:1045–1049.
29. Teillet F, Boumendjel A, Boutonnat J, Ronot X (2008) Flavonoids as RTK inhibitors and potential anticancer agents. *Med Res Rev* 28:715–745.
30. Lu H, Chang DJ, Baratte B, Meijer L, Schulze-Gahmen U (2005) Crystal structure of a human cyclin-dependent kinase 6 complex with a flavonol inhibitor, fisetin. *J Med Chem* 48:737–743.
31. Morita M, et al. (2008) Baicalein 5,6,7-trimethyl ether activates peroxisome but not mitochondrial fatty acid beta-oxidation. *J Inherit Metab Dis* 31:442–449.
32. Toullec D, et al. (1991) The bisindolylmaleimide GF 109203X is a potent and selective inhibitor of protein kinase C. *J Biol Chem* 266:15771–15781.
33. Blanquart C, et al. (2004) The protein kinase C signaling pathway regulates a molecular switch between transactivation and transrepression activity of the peroxisome proliferator-activated receptor alpha. *Mol Endocrinol* 18:1906–1918.
34. Meyer MC, Kell PJ, Creer MH, McHowat J (2005) Calcium-independent phospholipase A2 is regulated by a novel protein kinase C in human coronary artery endothelial cells. *Am J Physiol Cell Physiol* 288:C475–C482.
35. Hubbard WC, et al. (2009) Newborn screening for X-linked adrenoleukodystrophy (X-ALD): Validation of a combined liquid chromatography-tandem mass spectrometric (LC-MS/MS) method. *Mol Genet Metab* 97:212–220.
36. Counter CM, et al. (1998) Telomerase activity is restored in human cells by ectopic expression of hTERT (hEST2), the catalytic subunit of telomerase. *Oncogene* 16:1217–1222.
37. Hopert A, Uphoff CC, Wirth M, Hauser H, Drexler HG (1993) Mycoplasma detection by PCR analysis. *In Vitro Cell Dev Biol Anim* 29A:819–821.
38. Braverman N, et al. (2000) PEX7 gene structure, alternative transcripts, and evidence for a founder haplotype for the frequent RCDP allele, L292ter. *Genomics* 63:181–192.
39. Roscher A, et al. (1985) The cerebrohepatorenal (Zellweger) syndrome: An improved method for the biochemical diagnosis and its potential value for prenatal detection. *Pediatr Res* 19:930–933.